Cyril Fernando Memorial Oration

Diagnosis of Alzheimer's disease: a question of channels?

H A de Silva*

Journal of the Ceylon College of Physicians, 1998, **31**; 1 & 2, 16-30

Introduction and Background

People in both developed and developing nations are living longer than ever before. In industrialised nations, during this century alone, average life expectancy from birth has increased by more than 25 years. Indeed, the most rapidly growing age group in many countries comprises those aged 80 and above. People over 60 currently constitute a fifth of the British population, but will be a third by 2030. In 1951 Britain had 300 people aged over 100; by 2030 it will have 34,000. Furthermore, by the year 2030 it is estimated that between 17 and 20% or about 50 million of the US population will be over the age of sixty five[1]. Unfortunately, the developing world has not enjoyed the same revolutionary increase in longevity. None the less, 60% of people aged 60 and older live in developing countries – which have huge populations – and this percentage is expected to rise to 80% towards the middle of the next century. In Sri Lanka too, declining fertility rates and increasing life expectancy have inevitably lead to an increase in the population share of the elderly. Thus, the percentage of the population aged over 60 years in this country is expected to increase rapidly from 8% currently, to reach 13% in 2010, and 21% in 2025[2], and is thought to have the fastest ageing population in the world.

Dementia, defined as a syndrome of cognitive and emotional impairment severe enough to interfere with daily function and quality of life, is one of the most distressing and burdensome health problems of the elderly and those who care for them. Longer lifespans and increasing knowledge of the causes of cognitive decline, particularly Alzheimer's disease, have led to the prediction of dementia as an epidemic extending into the 21st century. Alzheimer's disease, the most common cause of dementia in the developed world, affects almost 1 in 10 individuals who survive beyond the age of 65. It is the fourth leading cause of death in Western countries, preceded only by heart disease, cancer and stroke[3]. With advancing age, the prevalence of the disease increases to an estimated 19% for individuals 75-85 years old and greater than 45% for individuals over 85[4]. There are currently 2.5 to 4 million Alzheimer's disease patients in the US, and 17 to 25 million worldwide[5]. The annual cost for caring for these patients, in the United States alone, is estimated at more than US $ 100 billion[6]. Other data show that for every demented patient there are approximately eight non-demented individuals with cognitive deterioration that adversely affects their quality of life[7]. Consequently, a staggering number of elderly people with mild to severe cognitive impairment, perhaps 30 to 40 million, can be expected in the next 35 years, representing a great human and economic toll.

Diagnosis of Alzheimer's disease

Alzheimer's disease (AD), first described by Alois Alzheimer in 1906[8], is a neurodegenerative disease of the central nervous system (CNS) and is characterized by progressive loss of cognitive ability, severe behavioural abnormalities and ultimately death[9]. This cognitive decline is presumably the consequence of the synaptic loss and extensive neuronal cell death that occur in regions of the brain involved in cognition and memory, principally the medial temporal lobe[9]. Three characteristic neuropathological lesions have been found in these regions: intracellular neurofibrillary tangles composed of abnormal cytoskeletal proteins; shrinkage and loss of cholinergic projection neurones; and extracellular deposition of complex protein deposits, called μ-amyloid (Aβ)[9].

The progressive deposition of Aβ in the brain, principally in the medial temporal lobe, is the pathological hallmark of AD, and appears to precede

* *Senior Lecturer & Head Department of Pharmacology, Faculty of Medicine, University of Kelaniya.*

the onset of dementia by many years[9]. Thus, Aβ deposition is thought to start a cascade of events (amyloid cascade hypothesis) that finally results in the clinical symptomatology of dementia that brings the patient to the physician.

The diagnosis and assessment of dementia is still largely based upon clinical and neuropsychological criteria and AD, in particular, is usually diagnosed by exclusion of other known causes of dementia. There is currently no blood test, CSF test, peripheral biochemical marker, or simple biopsy that allows for the definitive diagnosis of AD to be made during life. As a result, a definitive diagnosis of this disorder can be made only if histologic confirmation is obtained by performance of a cerebral biopsy or an autopsy. However, in the absence of such histopathological analysis, a diagnosis of "probable" AD can be made after extensive neurological and neuropsychological testing. Clinicians must therefore rely on clinical diagnostic criteria for AD, the two most widely used of which are those of the Diagnostic and Statistical Manual of Mental Disorders (DSM – IV)[10] and those of the National Institute of Neurological and Communicative Disorders and Stroke and the Alzheimer's Disease and Related Disorders Association Work Group (NINCDS-ADRDA)[11], which include recommended laboratory and brain imaging studies. To assess patients in relation to the criteria for the diagnosis of probable AD, physicians must perform formal mental status testing in addition to careful history taking and physical, psychiatric, and neurologic examinations. The laboratory tests required include a CT scan, a chest X-ray, an electroencephalogram, a comprehensive biochemical screening, determination of the vitamin B_{12} level, thyroid function tests, a serologic test for syphilis, and if suggested by other findings, an examination of the cerebrospinal fluid.

However, when compared against the "gold standard" of pathologic AD, their diagnostic accuracy in dementia of the Alzheimer type varies widely, the average being about 75%, with false positive rates ranging from more than 50% down to 11%[12] for a maximum sensitivity or detection rate of approximately 90%[12]. Currently, AD may be incorrectly diagnosed clinically in as many as 25 to 40% of cases in non-research diagnostic settings[4]. Therefore, the importance of identifying a biochemical marker of this disease in easily accessible cells such as platelets or erythrocytes is obvious: firstly as a guide to diagnosis in life and, secondly, for monitoring the progression of the disease and the effectiveness of any therapy. This dilemma has fuelled the search for an accurate and simple diagnostic tool for AD, for example, something on the level of a pregnancy test.

Platelets and potassium channels as possible markers for AD

In 1989, Joachim et al[13] found Aβ deposits in the skin, subcutaneous tissue, and intestine of patients with AD, suggesting that the process underlying Aβ deposition in AD may be a generalized disturbance, instead of an alteration restricted to the brain. This opened the possibility to find a marker of the disease outside the brain. Interestingly, platelets are the major circulating repository of β-APP, the precursor of Aβ[14], representing a probable candidate. A number of abnormalities in the platelets of AD patients, such as increased membrane fluidity[15], and disordered intracellular Ca^{2+} homeostasis[15] have been reported. These abnormalities were more severe in those who carry the ApoE4 allele[16], which has been shown to be genetically associated with the common late-onset sporadic form of AD[17]. Thus, platelets are a potential source of the amyloid deposits in brain parenchyma and meningeal blood vessels, and may be an important non-neural cell with which to study the pathogenesis of AD.

Furthermore, various abnormalities of K^+ fluxes, particularly of K^+ channels, have been described in neural and non-neural cells from patients with AD[18] (see below). Therefore, since AD is considered a systemic process involving multiple organ systems and since K^+ channel abnormalities have been reported in non-neural cells, I investigated the pharmacology of K^+ channels in human platelets as a possible site for AD pathology.

As a first step, I characterized Na^+/K^+ pumps and K^+ channels (the principal K^+ transport systems in mammalian cells) in platelets from young healthy volunteers, in order to provide a comparative bacground for the use of similar studies on platelets from patients with AD.

Potassium transport systems in normal human platelets

The sodium/potassium pump

The Na^+/K^+ pump (the Na^+/K^+ activated adenosine triphosphatase, Na^+/K^+ ATPase), operationally defined by its susceptibility to inhibition by cardiotonic steroids such as ouabain and digoxin, is the mechanism that contributes most to the maintenance of Na^+ and K^+ gradients across the cell membrane, and the majority (80-90%) of K^+ influx in human cells is mediated by this pump[19]. It uses the energy of the hydrolysis of ATP to pump two K^+ ions in and three Na^+ ions out of the cell at each cycle, and as a result the pump is electrogenic[19]. Both of these ions are transported against their concentration gradients, and this keeps the intracellular concentration of K^+ high and the intracellular concentration of Na^+ low, which plays an important role in the maintenance of cell resting potential.

Methods

The activity of Na^+/K^+ pumps in intact cells can be studied by measuring the uptake of radio-labelled rubidium ($^{86}Rb^+$, used as a radioactive substitute for K^+)[20], as demonstrated in a variety of tissues. Furthermore, the uptake of $^{86}Rb^+$ into cells is sensitive to low concentrations of cardiac glycosides such as ouabain, and this has been used as a method for demonstrating the presence of Na^+/K^+ pumps in the cell membrane[21].

Venous blood was obtained from healthy volunteers, and platelets were prepared by ultracentrifugation. Samples of platelets ($0.5X10^8$ platelets / 200 µl) were put into two sets of incubation tubes (in triplicate) and incubated with a tracer concentration of (a) with ouabain 100 µM (b) without ouabain, in Krebs solution (control). At the end of the incubation the cells were lysed and the amount of $^{86}Rb^+$ taken up was measured by liquid scintillation counting.

Results

The uptake of $^{86}Rb^+$ in control samples was taken as the total uptake. The differences between total uptake and the uptake in ouabain treated samples was taken as ouabain-sensitive uptake.

In previous studies on erythrocytes, ouabain at a maximally effective concentration of 100 µM achieved 90% inhibition of $^{86}Rb^+$ uptake[21]. In my experiments, ouabain (100µM) inhibited the $^{86}Rb^+$ uptake by about 85% (Figure 1).

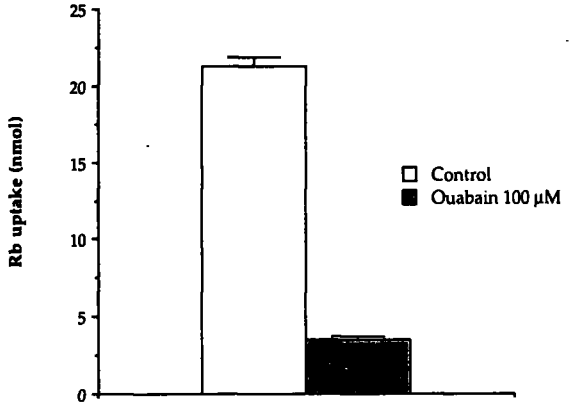

Figure 1. The effect of ouabain on $^{86}Rb^+$ uptake. The experiments were conducted in triplicate, n=11.

Comment

In these experiments, ouabain-sensitive $^{86}Rb^+$ uptake (corresponding to the activity of Na^+/K^+ pumps) contributed about 85% to the total uptake in human platelets. This value is similar to that determined in other cell types[21], and confirms the presence Na^+/K^+ pumps in the human platelet, and also that most of the K^+ (Rb^+) transport into the platelet occurs via these pumps.

Potassium channels

K^+ channels are present in all mammalian cells and are exceptionally diverse in both variety and function. They exist in several subtypes, multiple subtypes often being present in a single cell[22]. When opened, these channels permit the efflux of K^+ bacause of the large K^+ gradient across the cell membrane. They therefore lead to the outward flux of positive charge, and this tends to oppose depolarization, causing repolarization or hyperpolarization.

Based on their gating, conductance, and pharmacological characteristics (sensitivity to animal toxins such as, apamin, charybdotoxin, iberiotoxin, and dendrotoxin) K^+ channels are

currently classified into four basic groups. However, within this classification, subtypes of K^+ channels usually exist, and some exhibit overlapping characteristics[23];

1) voltage-dependent K^+ (K_v) channels
2) Ca^{2+}-activated K (K_{Ca}) channels,
3) receptor-coupled K^+ channels, and
4) other K^+ channels - adenosine 5'-triphospate (ATP)-dependent K^+ (K_{ATP}) channels, Na^+-activated K^+ (K_{Na}) channels, and volume-sensitive K^+ (K_{vol}) channels.

The activity of K_{Ca} channels increases in response to an increase in intracellular Ca^{2+}. The hyperpolarization that results from increased activity of these channels thus constitutes an important feedback mechanism for the regulation of voltage-dependent Ca^{2+} entry. They can be divided into three main classes on the basis of their single-channel conductances and selectivity to naturally-occurring animal toxins[24]: large conductance channels (BK_{Ca} channels, sensitive to iberiotoxin isolated from the Asian scorpion venom); charybdotoxin-sensitive channels with intermediate conductance (K_{Ch} channels, sensitive to charybdotoxin isolated from the Israeli scorpion venom); and small-conductance channels (SK_{Ca} channels, sensitive to apamin isolated from bee venom).

Voltage-dependent K^+ (K_v) channels form the largest and the most diverse class of ion channels. They are specifically inhibited by α-dendrotoxin, a peptide isolated from the venom of the green mamba snake. All K_v channels serve the same basic function, i.e. to create or stabilize a negative membrane potential, counteracting the depolarizing effects of channels that pass Na^+ or Ca^{2+}. Therefore, K_v channels open when the cell is depolarized, and the resultant K^+ efflux through these channels increases with depolarization through this voltage-dependent activation[25].

The platelet membrane maintains large ionic gradients of Na^+ and K^+ and has a negative resting membrane potential similar to that in other cells[26]. As described above, K^+ efflux through K^+ channels hyperpolarizes the cell membrane in response to depolarizing stimuli. There are K^+ channels in platelets, which may serve this function. Based on the observation that Rb^+ efflux can be stimulated by agonists such as thrombin and ionomycin (see below) from platelets that have been preloaded with $^{86}Rb^+$[20], and using selective inhibitors of K^+ channels to inhibit these stimulated $^{86}Rb^+$ effluxes, I characterized three types of K^+ channels in normal human platelets[27].

Methods

The platelets from healthy volunteers were prepared as described previously, by loading fresh platelets with $^{86}Rb^+$ and stimulating $^{86}Rb^+$ efflux with platelet agonists, thrombin and ionomycin[28].

Briefly, blood was drawn by venepuncture from healthy volunteers and anticoagulated with acid-citrate-dextrose (ACD). Platelets were prepared by centrifugation and loaded with $^{86}Rb^+$. The platelet suspension (2.5×10^7 platelets per ml) was then injected into perfusion chambers and the cells were immobilized on inert filters. Thereafter, the platelets were continuously perfused with Krebs solution (physiological buffer), to allow them to stabilize on the filters for 20 min before the start of each experiment. When presenting efflux results, I have referred to the starting point of the perfusion as time -20 and therefore, the platelet stabilization period (20 min) will be from time -20 to time 0. During this time the perfusate was collected at 2 min intervals.

After this (time 0) the perfusion was changed for 5 min (from 0-5 min of the experiment; indicated by the horizontal bar in figures 2-5) to Krebs solution containing thrombin (0.3 IU/ml) or ionomycin (1 μM). During this time the perfusate was collected at 1-min intervals. The perfusion was then continued with the original solution for another 20 min. The total experimental period was 50 min; from time -20 to time 30. The solutions used for perfusion were bubbled with 95% O_2 and 5% CO_2 throughout the experiment (pH 7.4).

At the end of the experiment (at 30 min) the polycarbonate filters were retrieved and placed in scintillation vials, to which scintillation fluid was added. The radioactivity in the perfusates and filters was determined by liquid scintillation counting in a radio-activity counter and the loss of radioactivity from the cells was calculated. The amount of $^{86}Rb^+$ (pmol) in each fraction of perfusate collected was determined using the specific activity of the isotope.

The radioactivity was measured in each fraction and plotted as a function of time. The results were expressed as the cumulative efflux of $^{86}Rb^+$ (from 0-14 min of the experimental period; time after stimulation of the platelets) against time.

Results

The results are shown in Figures 2-5 as cumulative effluxes of $^{86}Rb^+$ from 0-14 min and are summarized in Table 1 as the percentage inhibition of the maximum cumulative efflux by the different inhibitors used.

When the platelets were perfused with Krebs solution there was a linear cumulative efflux with time (open circles; Figures 2-5). This efflux, which shall be referred to as the non-stimulated efflux, is attributable to another K^+ transport system, the $Na^+/K^+/2Cl^-$ co-transporter, present in human platelets[28].

Thrombin (0.3 IU/ml), perfused over the platelets for 5 min (from 0-5 min of the experiment) stimulated an increase in the cumulative $^{86}Rb^+$ efflux from the cells (Figure 2). As shown below, this efflux, which I shall call the thrombin-stimulated efflux, is mediated via two types of K_{Ca} channels and a K_v channel.

Apamin (100 nM) and charybdotoxin (300 nM) inhibited thrombin-stimulated $^{86}Rb^+$ efflux ($p < 0.0001$) (Figure 2). Apamin (100 nM) and charybdotoxin (300 nM) added together resulted in a greater effect than when either was added alone ($p < 0.0001$) (Figure 2).

α-dendrotoxin (100-200 nM) inhibited the thrombin-stimulated $^{86}Rb^+$ efflux in a concentration-dependent manner ($p < 0.0001$) (Figure 3). Furthermore, α-dendrotoxin (200 nM) added together with apamin (100 nM) and charybdotoxin (300 nM) resulted in a greater effect than when apamin and charybdotoxin were added together ($p < 0.0001$) (Figure 4).

The calcium ionophore ionomycin (1 μM), perfused over the platelets for 5 min (from 0-5 min of the experiment), stimulated an increase in the cumulative $^{86}Rb^+$ efflux from the cells (Figure 5). Apamin (100 nM) and charybdotoxin (300 nM) inhibited the ionomycin-stimulated $^{86}Rb^+$ efflux ($p < 0.0001$) (Figure 5). The two toxins added together resulted in a greater effect than when either was added alone ($p < 0.0001$) (Figure 5).

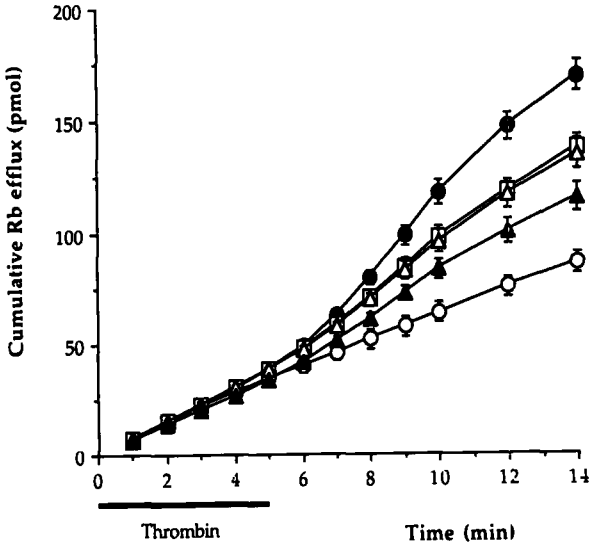

Figure 2. The effects of apamin and charybdotoxin on cumulative $^{86}Rb^+$ efflux. Thrombin 0.3 IU/ml (filled circles) stimulated an increase in cumulative $^{86}Rb^+$ efflux over the non-stimulated efflux (open circles). Apamin 100 nM (open squares) and charybdotoxin 300 nM (open triangles) inhibited the thrombin-stimulated $^{86}Rb^+$ efflux ($p < 0.0001$). Apamin (100 nM) and charybdotoxin (300 nM) added together (filled triangles) inhibited the thrombin-stimulated efflux more than when either toxin was added alone ($p < 0.0001$). Each experiment was conducted in duplicate (n=11-12).

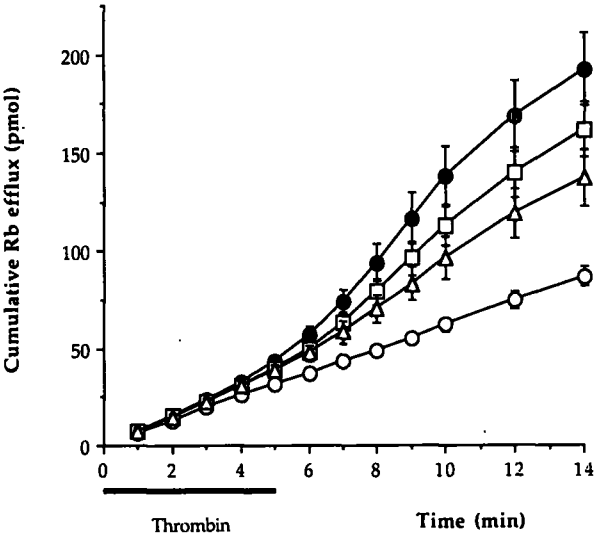

Figure 3. The effect of α-dendrotoxin on cumulative $^{86}Rb^+$ efflux. Thrombin 0.3 IU/ml (filled circles) stimulated an increase in cumulative $^{86}Rb^+$ efflux over the non-stimulated efflux (open circles). α-dendrotoxin 100 nM and 200 nM (open squares and open triangles respectively) inhibited the thrombin-stimulated $^{86}Rb^+$ efflux in a concentration-dependent manner ($p < 0.0001$). Each experiment was conducted in duplicate (n=12).

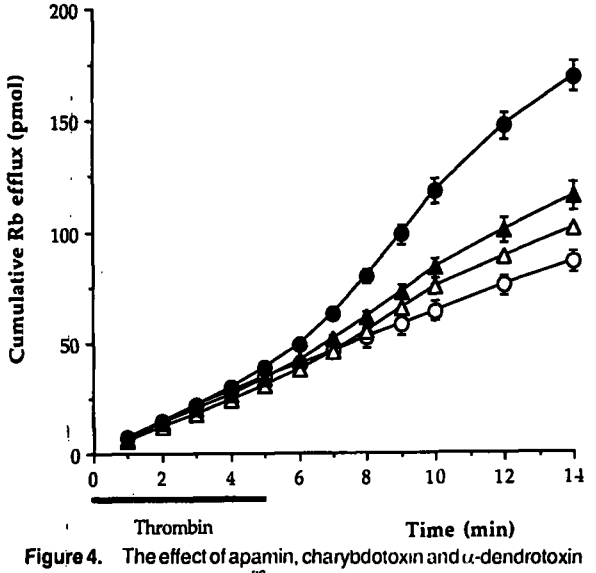

Figure 4. The effect of apamin, charybdotoxin and α-dendrotoxin on cumulative $^{86}Rb^+$ efflux. Thrombin 0.3 IU/ml (filled circles) stimulated an increase in cumulative $^{86}Rb^+$ efflux over the non-stimulated efflux (open circles). Apamin 100 nM, charybdotoxin 300 nM and α-dendrotoxin 200 nM added together (open triangles) inhibited thrombin-stimulated $^{86}Rb^+$ efflux more than apamin and charybdotoxin in combination (closed triangles) ($p < 0.0001$). Each experiment was conducted in duplicate (n=10-12). Error bars are not shown if smaller than the symbol.

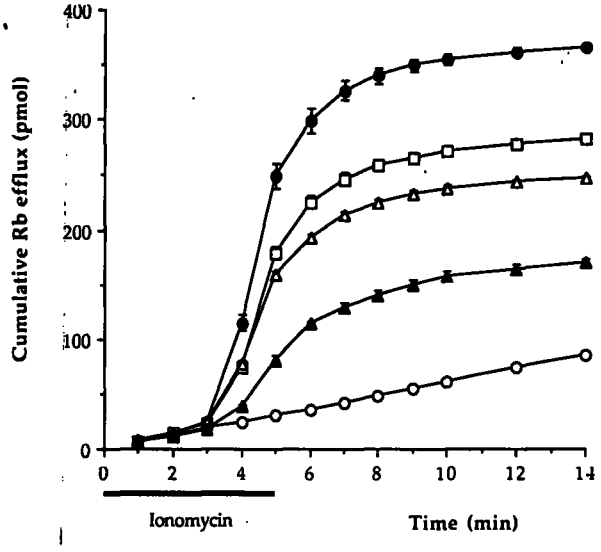

Figure 5. The effect of apamin and charybdotoxin on ionomycin-stimulated cumulative $^{86}Rb^+$ efflux. Ionomycin 1 μM (filled circles) stimulated an increase in cumulative $^{86}Rb^+$ efflux over the non-stimulated efflux (open circles). Apamin 100 nM (open squares) and charybdotoxin 300 nM (open triangles) inhibited the ionomycin-stimulated $^{86}Rb^+$ efflux ($p < 0.0001$). Apamin (100 nM) and charubdotoxin (300 nM) added together (filled triangles) inhibited the ionomycin-stimulated efflux more than when either toxin was added alone ($p < 0.0001$). Each experiment was conducted in duplicate (n=12). Error bars are not shown if smaller than the symbol.

Comment

Changes in intracellular Ca^{2+} play an important role during platelet activation[29]. Activation of these cells with thrombin and ionomycin stimulate a rapid increase in the cytoplasmic Ca^{2+} concentration, caused mainly by release of Ca^{2+} from intracellular stores[29]. This increase in cytoplasmic Ca^{2+} concentration is thought to open K^{Ca} channels, resulting in an efflux of K^+, which hyperpolarizes the cell membrane. On the other hand, activation of human platelets by agonists such as thrombin is followed by membrane depolarization[26]. Voltage-dependent K^+ channels (K_v channels) open when a cell is depolarized, and that results in the repolarization of the cell membrane.

In the experiments described above, thrombin and ionomycin stimulated $^{86}Rb^+$ efflux from $^{86}Rb^+$-loaded human platelets. The sensitivity of this efflux to inhibition by specific K_{Ca} channel inhibitors, apamin and charybdotoxin, suggests the presence of two types of K_{Ca} channels (SK_{Ca} and K_{Ch}). Also, apamin and charybdotoxin together had an approximately additive effect on thrombin- and ionomycin- stimulated $^{86}Rb^+$ efflux (Table 1), suggesting that the K_{Ca} channels that human platelets contain are independently sensitive to apamin and charybdotoxin.

α-dendrotoxin inhibited the thrombin-stimulated $^{86}Rb^+$ efflux in a concentration-dependent manner, suggesting the presence of K_v channels in human platelets. Furthermore, α-dendrotoxin added together with apamin and charybdotoxin had a greater effect on thrombin-stimulated $^{86}Rb^+$ efflux than any of these toxins alone and a greater effect than apamin and charybdotoxin combination (Table 1a). This provides evidence to suggest that normal human platelets contain at least three different types of K^+ channels (SK_{Ca}, K_{Ch} and K_v) which are independently sensitive to apamin, charybdotoxin, and α-dendrotoxin.

Having characterized Na^+/K^+ pumps and K^+ channels in platelets from healthy volunteers, I investigated $^{86}Rb^+$ fluxes from platelets of patients with AD and age-matched controls in order to determine whether Na^+/K^+ pumps and K^+ channels are abnormal in AD.

Table 1

(a) Thrombin-stimulated $^{86}Rb^+$ efflux

Inhibitor	% inhibition
Apamin (100 nM)	30 (29-34)
Charybdotoxin (300 nM)	33 (28-34)
Dendrotoxin (100 nM)	31 (29-35)
Dendrotoxin (200 nM)	45 (43-48)
Apamin (100 nM) + charybdotoxin (300 nM)	55 (51-58)
Apamin (100 nM) + charybdotoxin (300 nM)dendrotoxin (200 nM)	86 (84-88)

(b) Ionomycin-stimulated $^{86}Rb^+$ efflux

Inhibitor	% inhibition
Apamin (100 nM)	24 (19-25)
Charybdotoxin (300 nmol)	32 (30-35)
Apamin (100 nM) + charybdotoxin (300 nmol)	54 (49-57)

Table 1. Percentage inhibition of thrombin-stimulated and ionomycin-stimulated $^{86}Rb^+$ effluxes in platelets by apamin, charybdotoxin, and α-dendrotoxin. Data are given as median (range).

Abnormalities of potassium channels in the platelets of patients with Alzheimer's disease

K^+ channels (K_{Ca} channels in particular) change during the acquisition of memory in both molluscs and mammals[30], and memory loss is characteristic of AD[31]. The involvement of K^+ channels in the pathogenesis of age-related cognitive impairment was first suggested by Landfield and Pitler[32]. They observed an increased after-hyperpolarization in hippocampal slices of aged rats, which they attributed to altered Ca^{2+}-dependent K^+ conductance. Subsequently, several studies have shown K^+ channel abnormalities in both neural and non-neural cells. These include a functionally absent K^+ channel from cultured human fibroblasts from AD patients[33], and reduced binding of [125I]-apamin, a specific inhibitor of SK_{Ca} channels[24], to post-mortem hippocampal neurones in AD[34], suggesting that an anatomically discrete loss of K_{Ca} channels within the hippocampal formation occurs in AD.

The human platelet, which carries out a number of biochemical processes that also occur in the brain, has been proposed as a peripheral model for neurones. The demonstration of abnormalities of function and morphology pf platelets in Parkinson's disease[35], Huntington's disease[36], depression[37], and AD (see above), and the association between megakaryocytic leukaemia and Down's syndrome[38], suggests that disease-specific abnormalities in the brain could be reflected in the platelet.

In the study described here, I have studied $^{86}Rb^+$ fluxes from platelets of patients with AD and non-demented individuals of comparable age (age-matched controls), in order to determine whether those fluxes are abnormal in AD, and if so the nature of the abnormalities. I describe here that the platelets from patients with AD had significant differences in the pharmacology of their K^+ channels, compared with young volunteers age-matched controls[39].

Methods

Patients and controls

Subjects were recruited, after having been given a full explanation of the study protocol, by the Oxford Project To Investigate Memory and Ageing (OPTIMA): 14 patients with AD and 14 non-demented age- and sex-matched controls; each experiment was performed with platelets obtained from these individuals. Informed consent was obtained from those without cognitive deficit, and for those with a significant deficit it was given by a close relative.

Diagnosis of probable AD was made according to criteria of the National Institutes of Neurology and Communicative Disorders-Alzheimer's Disease and Related Disorders Association Work Group (NINCDS-ADRDA)[11] and criteria of the DSM-IIIR[10]. A detailed clinical and psychiatric history was taken from each subject, followed by a full physical examination of all systems, and blood tests to exclude identifiable metabolic causes of memory loss and dementia. Each subject underwent neuropsychological assessment with the Cambridge Mental Disorders of the Elderly Examination

(CAMDEX)[40]. The cognitive section, Cambridge Cognitive Examination (CAMCOG), includes sections for testing memory, praxis, language, attention, concentration, orientation, abstract thinking, and calculation and had a maximum score of 107. It also enables the derivation of the Mini Mental State Examination (MMSE)[41], which is scored out of 30. A score of less than 80 in the CAMCOG and of less than 24 in the MMSE was considered to indicate a significant cognitive deficit. In addition, screening specifically included temporal-lobe-oriented x-ray computed tomography (CT) and single-photon-emission computed tomography (SPET) regional cerebral blood flow scans of the brain[42]. Those with a diagnosis of probable AD had no evidence of any other significant metabolic or psychiatric process that was thought to contribute to the dementia and also had evidence of significant medial temporal lobe atrophy on CT, and a moderate or greater parietotemporal blood flow deficit on SPET.

In a previous necropsy-confirmed cohort, the use of these criteria, using CT and SPET changes alone, without taking into account the clinical history or cognitive profile, had a sensitivity of over 85% and a specificity of over 95%[43].

Controls were selected to be age- and sex-matched, had no evidence of cognitive dysfunction, i.e. their CAMCOG scores were over 79/108[40], complained of no memory problems, and did not have the combination of a minimum medial temporal lobe width on CT of less than the fifth centile for controls and a moderate or greater parietotemporal perfusion deficit on SPET.

Demographic and other details of the subjects are given in Table 2. Platelets from patients with probable AD and age-matched controls were prepared, and perfusion experiments were carried out as previously described. I was blind to the diagnoses. The study was conducted in the University Department of Clinical Pharmacology, Oxford, and was approved by the Central Oxford Research Ethics Committee.

Table 2

Measure	Alzheimer's disease (n=14	Controls (n=14)
Age (y)	69.4 (7.3)	68.5 (7.7)
Sex (M/F)	8/4	8/4
Systolic blood pressure (mmHg)	140 (6)	142 (21)
Diastolic blood pressure (mmHg)	85 (6)	80 (12)
Serum sodium (mM)	139 (3)	139 (2)
Serum potassium (mM)	3.9 (0.4)	4.0 (0.3)
Serum calcium (mM)	2.43 (0.10)	2.31 (0.13)
Serum urea (M)	5.5 (1.4)	6.6 (2.7)
Serum creatinine (μM)	104 (12)	103 (23)
Blood glucose (mM)	5.9 (2.0)	5.5 (1.1)
Platelet count ($\times 10^9$/l)	233 (57)	229 (61)
Haemoglobin (g/dl)	13.9 (1.0)	14.2 (1.1)
Mean red cell volume (fl)	89 (5)	90 (5)
White cell count ($\times 10^9$/l)	6.9(1.4)	6.4 (1.5)
Total plasma cobalamins (ng/l)	270 (88)	330 (133)

Table 2. Subject data. The data are given as mean (sd). There were no significant differences between the groups. Statistical comparisons by Student's unpaired t-test.

Results

Uptake of rubidium by platelets and non-stimulated $^{86}Rb^+$ efflux

The uptake of $^{86}Rb^+$ by the platelets was the same in both groups (Figure 6). Since about 85% of this uptake in platelets is attributable to the Na^+/K^+ pump (see above), this result suggests that the pump functions normally in AD. Furthermore, the non-stimulated cumulative $^{86}Rb^+$ efflux which is mediated by the $Na^+/K^+/2Cl^-$ co-transporter[28], was linear with time (open circles; Figures 7-12), and did not differ between AD patients and controls suggesting that this co-transporter too functions normally in AD.

Thrombin-stimulated $^{86}Rb^+$ efflux

Control subjects

In control subjects, thrombin stimulated an increase in $^{86}Rb^+$ efflux from platelets (Figures 7 and

9). In these subjects, apamin and charybdotoxin inhibited the thrombin-stimulated $^{86}Rb^+$ efflux by at least 18% and 16% respectively. When the data from all the control subjects were pooled, both apamin and charybdotoxin caused significant reductions in $^{86}Rb^+$ efflux (Figure 7; Table 3a). In addition, α-dendrotoxin inhibited thrombin-stimulated $^{86}Rb^+$ efflux from the platelets of the controls (Figure 9; Table 3a). These results are similar both qualitatively and quantitatively to the effects of these toxins on thrombin-stimulated $^{86}Rb^+$ efflux in the platelets of young volunteers[27].

Alzheimer's disease

Thrombin stimulated $^{86}Rb^+$ efflux from the platelets of patients with AD (Figures 8 and 10), to the same extent as in controls (cf. Figures 7 and 8). In contrast to the results in controls, apamin and charybdotoxin had minimal effects on thrombin-stimulated $^{86}Rb^+$ efflux (less than 4% inhibition) in patients with AD. When the data from all the patients with AD were pooled, neither apamin nor charybdotoxin caused significant reductions in $^{86}Rb^+$ efflux (Figure 8; Table 3a). In contrast, α-dendrotoxin inhibited the thrombin-stimulated $^{86}Rb^+$ efflux from the platelets of patients with AD (Figure 10; Table 3a).

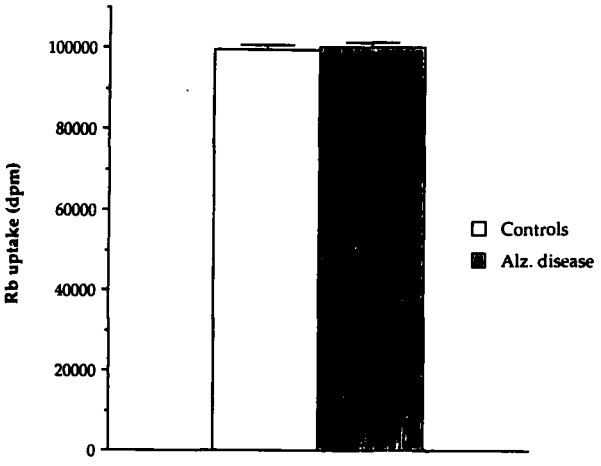

Figure 6. The uptake of by the platelets of patients with AD and by the platelets of age-matched controls. The results are expressed as mean (s.e. mean) and were compared using Student's unpaired t-test (n=12 in each group; $p > 0.1$)

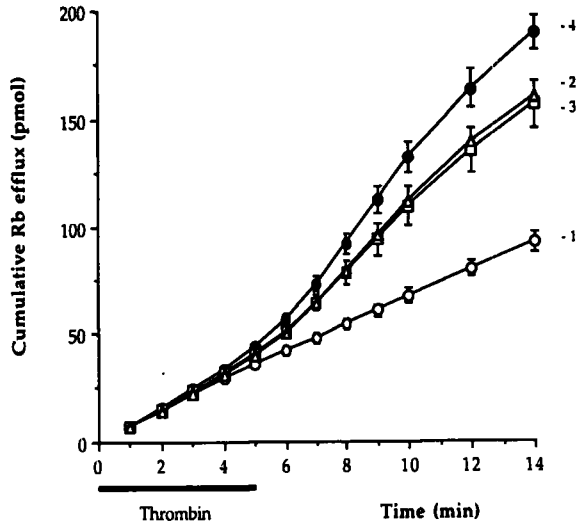

Figure 7. The effects of apamin and charybdotoxin on thrombin-stimulated $^{86}Rb^+$ efflux. Control subjects. Thrombin 0.3 IU/ml (4-filled circles) perfused over the platelets for 5 min (from 0-5 min of the experimental period, indicated by the horizontal bar) increased $^{86}Rb^+$ efflux over the non-stimulated efflux (1-open circles). Apamin 100 nM (3-open squares) and charybdotoxin 300 nM (2-open triangles) inhibited the stimulated $^{86}Rb^+$ efflux ($n=14$; $p < 0.0001$).

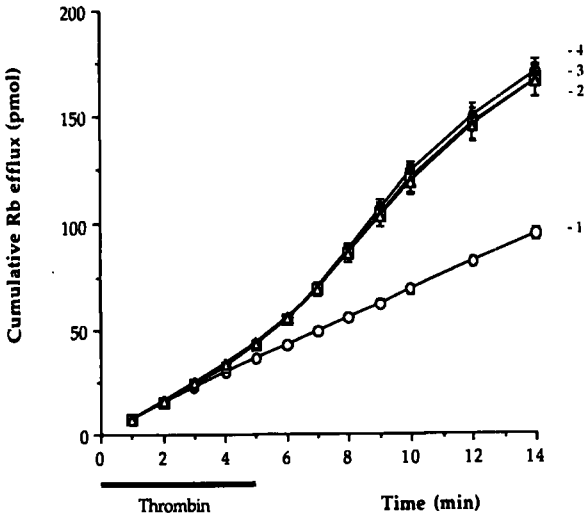

Figure 8. The effects of apamin and charybdotoxin on thrombin-stimulated $^{86}Rb^+$ efflux. Alzheimer's disease. Thrombin 0.3 IU/ml (4-filled circles) increased $^{86}Rb^+$ efflux over the non-stimulated efflux (1-open circles) to the same extent as in controls ($p=0.996$). Apamin 100 nM (3-open squares) and charybdotoxin 300 nM (2-open triangles) had no significant effect on the stimulated $^{86}Rb^+$ efflux ($n=14$; $p=0.941$).

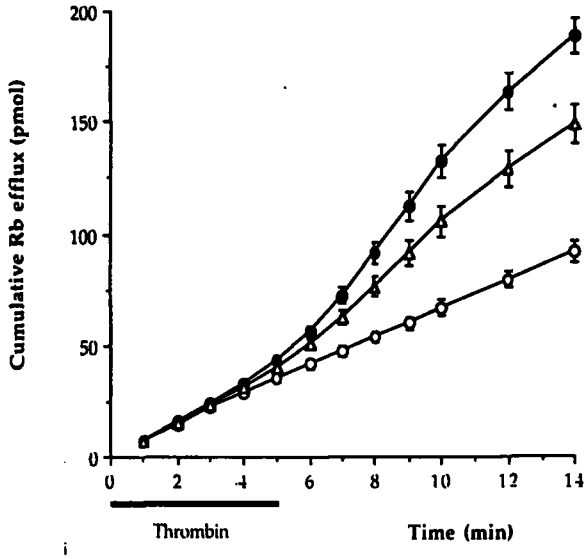

Figure 9. The effect of α-dendrotoxin on thrombin-stimulated $^{86}Rb^+$ efflux. Control subjects. Thrombin 0.3 IU/ml (filled circles) increased $^{86}Rb^+$ efflux over the non-stimulated efflux (open circles). α-dendrotoxin 200 nM (open triangles) inhibited the thrombin-stimulated efflux (n=14; $p < 0.0001$).

Table 3

(a) Thrombin-stimulated $^{86}Rb^+$ efflux

Toxin	Controls	Alzheimer's disease	P value
Apamin	26 (20-27)	0 (0-0)	< 0.01
Charybdotoxin	22 (18-29)	0 (0-3)	< 0.01
α-dendrotoxin	26 (20-29)	19 (18-27)	NS

(b) Ionomycin-stimulated $^{86}Rb^+$ efflux

Toxin	Controls	Alzheimer's disease	P value
Apamin	30 (20-31)	1 (0-2)	< 0.01
Charybdotoxin	28 (24-34)	4 (1-2)	< 0.01
Apamin + Charybdotoxin	51 (34-52)	2 (0-4)	< 0.01
Iberiotoxin	2 (0-3)	0 (0-4)	NS

Table 3. Inhibition of thrombin-stimulated and ionomycin-stimulated $^{86}Rb^+$ effluxes by apamin, charybdotoxin, α-dendrotoxin, and iberiotoxin in platelets of patients with AD and age- and sex-matched controls. Data are given as median (interquartile range) percentages. Statistical comparisons by rank sum tests.

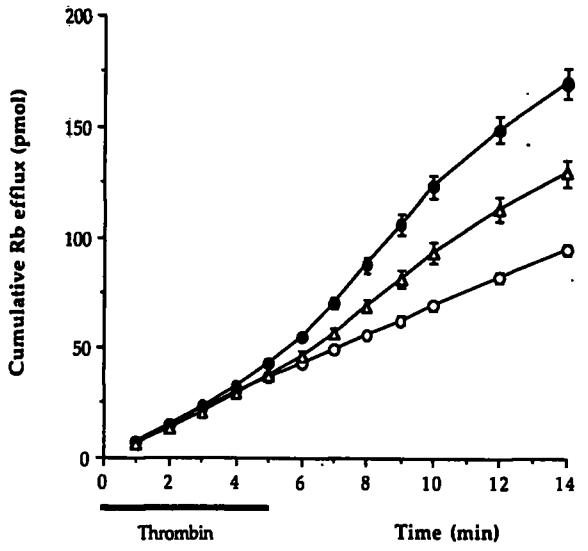

Figure 10. The effect of α-dendrotoxin on thrombin-stimulated $^{86}Rb^+$ efflux. Alzheimer's disease. Thrombin 0.3 IU/ml (filled circles) increased $^{86}Rb^+$ efflux over the non-stimulated efflux (open circles). α-dendrotoxin 200 nM (open triangles) inhibited the thrombin-stimulated efflux (n=14; $p < 0.0001$).

Ionomycin-stimulated $^{86}Rb^+$ efflux

Control subjects

In control subjects, apamin and charybdotoxin inhibited the ionomycin-stimulated $^{86}Rb^+$ efflux by at least 18% and 22% respectively. When the data from all the controls were pooled, both apamin and charybdotoxin caused significant reductions in $^{86}Rb^+$ efflux (Figure 11; Table 3b). The two toxins combined resulted in a greater effect than when either was added alone (Figure 11; Table 3b). These results are qualitatively and quantitatively similar to those seen in young volunteers[27].

Alzheimer's disease

Ionomycin stimulated $^{86}Rb^+$ efflux from the platelets of patients with AD (Figure 12), to the same extent as in controls (cf. Figures 11 and 12). However, apamin, charybdotoxin, and their combination had minimal effects on the ionomycin-stimulated $^{86}Rb^+$ efflux in patients with AD (less than 5% inhibition). When the data from all the patients with AD were pooled, apamin and charybdotoxin, either alone or in combination, had minimal effects on $^{86}Rb^+$ efflux (Figure 12; Table 3b).

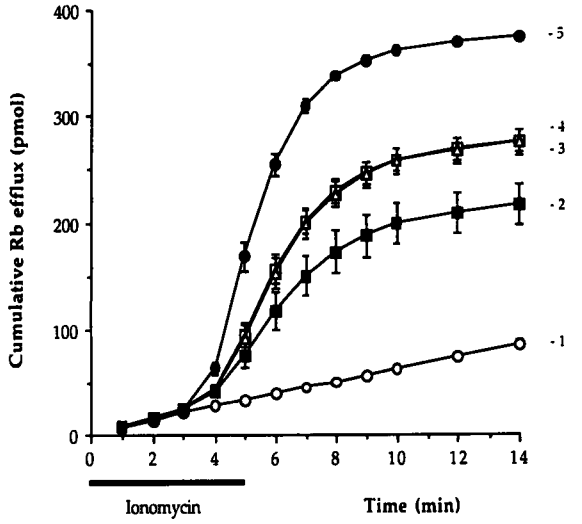

Figure 11. Effect of apamin and charybdotoxin on ionomycin-stimulated $^{86}Rb^+$ efflux. Control subjects. Ionomycin 1 μM (5-filled circles) increased $^{86}Rb^+$ efflux over the non-stimulated efflux (1-open circles). Apamin 100 nM (4-open squares) and charybdotoxin 300 nM (3-open triangles) inhibited the stimulated $^{86}Rb^+$ efflux ($p < 0.0001$). Apamin and charybdotoxin combined (2-filled squares) inhibited the stimulated efflux more than either toxin alone ($n=14$; $p < 0.0001$).

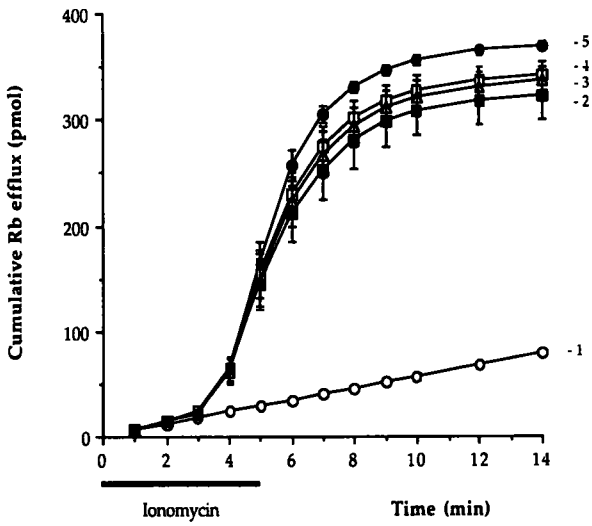

Figure 12. Effect of apamin and charybdotoxin on ionomycin-stimulated $^{86}Rb^+$ efflux. Alzheimer's disease. Ionomycin 1 μM (5-filled circles) stimulated $^{86}Rb^+$ efflux over the non-stimulated efflux (1-open circles) to the same extent as in controls ($p=0.960$). Apamin 100 nM (4-open squares) and charybdotoxin 300 nM (3-open triangles), either alone or in combination (2-filled squares), had no significant effect on the stimulated $^{86}Rb^+$ efflux ($n=14$; $p=0.883$).

Iberiotoxin had no effect on ionomycin-stimulated effluxes in platelets from any individual (Table 3b). This is similar to results in the platelets of young volunteers[27], and suggests that human platelets do not contain BK_{Ca} channels.

Comment

Although abnormalities of K^+ channels have been reported in AD in neural cells (reduced post-mortem binding of [^{125}I]-apamin to hippocampal neurones[34]) and in fibroblasts (absence of a 113 pS TEA-sensitive channel[33]) this study is the first to show functional K^+ channel abnormalities in the platelets of patients with AD. The $^{86}Rb^+$ effluxes in platelets in response to both thrombin and ionomycin were quantitatively normal in AD, and the thrombin-stimulated efflux showed normal sensitivity to inhibition with α-dendrotoxin, suggesting that the K_v channels are normal in platelets in AD. However, the lack of inhibition of both thrombin-stimulated and ionomycin-stimulated effluxes by apamin and charybdotoxin suggests either that the SK_{Ca} and K_{Ch} channels are not present in platelets in AD or, if they are present, that they are not sensitive to inhibition by these toxins.

SK_{Ca} and K_{Ch} channels may be present in the platelets of patients with AD, but unresponsive to inhibition. This would be consistent with the observation that the binding of [^{125}I]-apamin is reduced in post-mortem hippocampal neurones in AD[34]. This might be due to a change in the structure of the binding sites of the inhibitors. Alternatively, it might be due to an abnormality of the specific interaction of Ca^{2+} with the channels, since the efflux stimulated by ionomycin, which increases the intracellular concentration of Ca^{2+}, was not inhibitable. Furthermore, the Na^+/K^+ pump and K_v channels were not affected, suggesting that K_{Ca} channels are selectively impaired in AD.

Alternatively, the SK_{Ca} and K_{Ch} channels may not be present at all in AD. However, if that is so, then $^{86}Rb^+$ efflux must be occurring through other K^+ channels, since the thrombin-stimulated and ionomycin-stimulated effluxes were quantitatively normal. However, normal human platelets do not

contain BK_{Ca} channels[27], and iberiotoxin, a selective inhibitor of BK_{Ca} channels, had no effect on ionomycin-stimulated effluxes in platelets from any individual (Table 3b), while the only other type of K^+ channel that is found in platelets, K_v channels[27], responded normally to α-dendrotoxin. These observations argue against upregulation of other normal channels in AD. On the other hand, metabolites of the β-APP are capable of *de novo* formation of K^+ channels[44], which are insensitive to some inhibitors[18], and the $^{86}Rb^+$ efflux that was detected in AD might be via such channels.

Although the exact pathogenetic mechanisms involved in AD are unknown, mismetabolism of β-APP and abnormal deposition of Aβ are considered "central events" in the aetiology and pathogenesis of the disease[9]. Aβ may be directly toxic or may increase the vulnerability of neurones to external insults[9]. Several studies have shown that Aβ toxicity might involve disordering of intracellular Ca^{2+} homeostasis, particularly by increasing resting and/or stimulated intracellular Ca^{2+} concentrations($[Ca^{2+}]_i$). Chronic exposure of human cortical and rat hippocampal neurones to Aβ results in an increase in resting $[Ca^{2+}]_i$ and increased $[Ca^{2+}]_i$ responses to depolarization and excitatory amino acids[45]. More recently, it has been shown that Aβ increases cell excitability and causes a rise in $[Ca^{2+}]_i$ in hippocampal neurones[46]. Consistent with a $[Ca^{2+}]_i$-destabilizing mechanism of action of Aβ is the finding that basic fibroblast growth factor can protect hippocampal neurones against Aβ toxicity by preventing loss of $[Ca^{2+}]_i$ homeostasis[47]. Furthermore, cultured fibroblasts from patients with AD had higher bombesin-stimulated and bradykinin-stimulated increases in $[Ca^{2+}]_i$ compared with those from healthy controls[48]. Also, platelets from patients with AD had a higher thrombin-stimulated rise in $[Ca^{2+}]_i$[15]. Increased $[Ca^{2+A}]_i$ can alter cell function and lead to cell damage by multiple pathways, including induction of apoptosis, abnormal membrane permeability, damage to the cytoskeleton, protein phosphorylation, and production of free radicals[9]. Interestingly, the toxicity of Aβ was not ameliorated by L-type Ca^{2+} channel blockers[9], indicating some specificity in the actions of Aβ on Ca^{2+} metabolism. In this context, the absence or non-functionality of the K_{Ca} channels might explain the observation that platelets from patients with AD had higher stimulated rises in $[Ca^{2+}]_i$, which might represent an exaggerated attempt to switch on non-existent or non-functional channels. The absence or non-functionality of K_{Ca} channels may lead to increased intracellular Ca^{2+} accumulation in these cells, thus beginning a cascade of subsequent cellular responses that eventually results in abnormal processing of β-APP and increased production of Aβ.

If the results described here are supported by further testing, K_{Ca} channel abnormalities in platelets might provide a surrogate marker for similar abnormalities of ion channels in the brains of patients with AD and might also provide a diagnostic marker for AD. Furthermore, if further research proves that K^+ channel abnormalities induced by β-APP and its metabolites are responsible for the neurotoxicity observed in AD, drugs that modulate K^+ channel activity could form the basis of a therapeutic treatment. K^+ channel activators have been shown to protect neurones against oxidative injury and Aβ toxicity[49], whilst some metabolites of β-APP itself, by activating K^+ channels, might also be neuroprotective[44]. Interestingly, tacrine a drug with anticholinesterase activity used to treat AD, can also modulate K^+ channels[50]. Tacrine blocks the slow outward K^+ current in neurones and blocks delayed outward and inward rectifying K^+ channels[50]. From this perspective, the pharmacological modulation of K^+ channels represents a rational therapeutic target in AD.

Conclusion

Alzheimer's disease represents an increasing financial and healthcare burden to society. Despite increasing knowledge of the pathological processes underlying AD, there are at present no biochemical markers for the definitive diagnosis of the disease. Accurate diagnosis is essential to initiate appropriate treatments and to provide information about prognosis and factors that may affect the course of

the disease. Therefore, the importance of identifying a peripheral marker of this disease in cells such as platelets or erythrocytes cannot be understated. Furthermore, despite the large amount of research devoted to discovering the causes and pathogenesis of AD, we are a long way from achieving such goals. However, the common denominator in the pathophysiology of this devastating disease appears to be the β-amyloid peptide.

Recently, β-APP and its amyloidogenic metabolic fragments have been shown to alter cellular ionic activity, either through interaction with existing ion channels or by *de novo* channel formation, and such alteration of ion channels, particularly of K^+ channels, has been linked with cellular toxicity underlying the neurodegeneration seen in AD.

Several abnormalities have been reported in the platelets of patients with AD, and platelets are the major circulating repository of β-amyloid. In addition, abnormalities of K^+ channels in non-neural cells such as skin fibroblasts taken from patients with AD have been demonstrated. Therefore, I investigated the pharmacology of K^+ channels in human platelets as a possible site for AD pathology, and have shown that Ca^{2+}-activated K^+ channels in platelets are selectively impaired in AD. This might provide a diagnostic marker for the disease and might also provide a short cut to the understanding of its cause.

Finally, medical treatment of AD is in its infancy. Therefore, one of the most important goals in current AD research is the development of a therapeutic regimen that will prevent, slow, or stop the neurodegenerative process. Interestingly, K^+ channel activators have been shown to protect neurones against β-amyloid toxicity, and tacrine, a drug used in the treatment of Alzheimer's disease, may act by modulating K^+ channels. Given the possibility that the beneficial effects of tacrine and other drugs on Alzheimer's disease are mediated via modulation of K^+ channels, platelet Ca^{2+}-activated K^+ channels may become a new target for future anti-Alzheimer's disease drug development.

References

1. Schoenberg BS. Epidemiology of Alzheimer's disease and other dementing disorders. *J Chron Dis* 1986; **39**: 1095-104.
2. De Silva WI. 1997. Population projections for Sri Lanka: 1991-2041. Research Studies Human Resource Development Series II. Sri Lanka: Institute of Policy Studies.
3. Bush TL, Miller SR, Criqui MN, et al. Risk factors for morbidity and mortality in older population: an epidemiological approach. In: Hazzard WR, Bierman EL, Blass JP, et al., ed. Principles of geriatric medicine and gerontology. McGraw Hill, New York. 1994; 153-66.
4. Evans DA. Prevalence of Alzheimer's disease in a community population of older persons. *J Am Med Assoc* 1989; **262**: 2551-6.
5. Keefover RW. The clinical epidemiology of Alzheimer's disease. *Neuroepidemiology* 1996; **14**: 337-51.
6. Ernst RL, Hay JW. The US economic and social costs of Alzheimer's disease revisited. *Am J Public Health* 1994; **84**: 1261-1264.
7. Larrabee GJ, Crook TH. Estimated prevalence of age-associated memory impairment derived from standardized tests of memory function. *Int Psychogeriatr* 1994; **6**: 95-104.
8. Alzheimer A. Uber einen eigernartigen schweren Erkrangkungsproze β der Hirurinde. *Neurologisches Centralblatt* 1906; **23**: 1129-36.
9. Yankner BA. Mechanisms of neuronal degeneration in Alzheimer's disease. *Neuron* 1996; **16**: 921-32.
10. American Psychiatric Association. Diagnosis and statistical manual of mental disorders. Fourth ed. Washington: American Psychiatric Association, 1994.
11. McKhann G, Drachman D, Folstein M, et al. Clinical diagnosis of Alzheimer's disease: report of the NINCDS-ADRDA work group under the auspices of Department of Health and Human Services Task Force on Alzheimer's Disease. *Neurology* 1984; **34**: 939-44.
12. Homer AC, Honavar M, Lantos PL, et al. Diagnosing dementia: do we get it right? *Br Med Journal* 1988; **297**: 894-896.
13. Joachim CL, Mori H, Selkoe DJ. Amyloid β-protein deposition in tissues other than brain in Alzheimer's disease. *Nature* 1989; **341**: 226-30.

14. Van Nostrand WE, Schmaier AH, Farrow JS, Cunningham DD. Protease nexin-II (amyloid beta-protein precursor): a platelet alpha granule protein. *Science* 1990; **248**: 745-8.

15. Hajimohammadreza I, Brammer MJ, Eagger S, Burns A, Levy R. Platelet and erythrocyte membrane changes in Alzheimer's disease. *Biochim Biophys Acta* 1990; **1025**: 208-14.

16. Davies TA, Long HJ, Rathbun WH, et al. Platelets from patients with Alzheimer's disease or ther dementias exhibit disease-specific and apolipoprotein E correlatable defects. *Int J Exp Clin Invest* 1996; **3**: 13-9.

17. Strittmatter WJ, Saunders AM, Schmechel D, Pericak-Vance M, Enghild J, Salvesen GS, Roses AD. Apolipoprotein E: high avidity binding to β-amyloid and increased frequency of type 4 allele in late-onset familial Alzheimer's disease. *Proc Natl Acad Sci USA* 1993; **90**: 1977-81.

18. Fraser SP, Suh Y-H, Djamgoz MBA. Ionic effects of the Alzheimer's disease β-amyloid precursor protein and its metabolic fragments. *Trends Neurosci* 1997; **20**: 67-72.

19. Glynn IM, Karlish JD. The sodium pump. *Ann Rev Physiol* 1975; **37**: 13-55.

20. Andersson TGL, Vinge E. The efflux of $^{86}Rb^{+}$ and [^{3}H]5-HT from human platelets during continuous perfusion: effects of potassium-induced membrane depolarization and thrombin stimulation. *Acta Physiol Scand* 1991; **141**: 421-8.

21. Andersson TLG, Vinge E. Effects of ouabain on ^{86}Rb-uptake, ^{3}H-5-HT-uptake and aggregation by 5-HT and ADP in human platelets. *Pharmacol Toxicol* 1988; **62**: 172-76.

22. Latorre R, Miller C. Conductance and sensitivity in potassium channels. *J Memb Biol* 1983; **71**: 11-30.

23. Watson S, Girdlestone D. Receptor & Ion Channel Nomenclature Suppl. *Trends Pharmacol Sci* 1996; 72-77.

24. Haylett DG, Jenkinson DH. Calcium-activated K^{+} channels. In: Potassium channels: structure, classification, function and therapeutic potential 1990; ed. Cook NS, pp. 70-95. Chichester: Ellis Horwood.

25. Hille B. Ionic channels of excitable membranes. 1991; Second ed. Sunderland MA: Sinauer.

26. Pipili E. Platelet membrane potential: simultaneous measurement of diSC3(5) fluorescence and optical density. *Thromb Haemostasis* 1985; **54**:

27. De Silva HA, Carver JG, Aronson JK. Pharmacological evidence of calcium-activated and voltage-gated potassium channels in human platelets. *Clin Sci* 1997; **93**: 249-255.

28. De Silva HA, Carver JG, Aronson JK. Effects of high external concentrations of potassium of ^{86}rubidium efflux in human platelets: evidence for $Na^{+}/K^{+}/2Cl^{-}$ co-transport. *Clin Sci* 1996; **91**: 725-731.

29. Rink TJ, Sage SO. Calcium signalling in human platelets. *Ann Rev Physiol* 1990; **52**: 431-49.

30. Etcheberrigaray R, Matzel DI, Lederhendler I, Alkon DL. Classical conditioning and protein kinase C activation regulate the same single potassium channel in *Hermissenda crassicornis* photoreceptors. *Proc Natl Acad Sci USA* 1992; **89**: 7184-8.

31. Katzman R. Alzheimer's disease. *New Engl J Med* 1986; **314**: 964-7.

32. Landfield PW, Pitler TA. Prolonged Ca^{2+}-dependent afterhyperpolarizations in hippocampal neurones of aged rats. *Science* 1984; **226**: 1089-92.

33. Etcheberrigaray R, Ito E, Oka K, et al. Potassium channel dysfunction in fibroblasts identifies patients with Alzheimer's disease. *Proc Natl Acad Sci USA* 1993; **90**: 8209-13.

34. Ikeda M, Dewar D, McColloch J. Selective reduction of [125I] apamin binding sites in Alzheimer hippocampus: a quantitative autoradiographic study. *Brain Res* 1991; **567**: 51-6.

35. Barbeau A, Campanella G, Butterworth RF, Yamada K. Uptake and efflux of ^{14}C-dopamine in platelets: evidence for a generalized defect in Parkinson's disease. *Neurology* 1975; **25**: 1-9.

36. Aminoff MJ, Trenchard A, Turner P, Wood WG, Hills M. Plasma uptake of dopamine and 5-hydroxytryptamine and plasma acetylcholine levels in patients with Huntington's chorea. *Lancet* 1974; **2**: 1115-6.

37. Garcia-Sevilla JA, Zis AP, Hollingsworth PJ, et al. Platelet α2- adrenergic receptors in major depressive disorder – binding of tritiated clonidine before and after tricyclic antidepressant drug treatment. *Arch Gen Psychiat* 1981; **38**: 1327-38.

38. Lewis DS, Thompson M, Hudson E, et al. Down's syndrome and acute megakaryoblastic leukaemia. *Acta Haematol* 1983; **70**: 236-42.

39. De Silva HA, Aronson JK, Grahame-Smith DG, Jobst KJ, Smith AD. Abnormal function of potassium channels in the platelets of patients with Alzheimer's disease. *Lancet* 1998; **352**: 1590-1593.

40. Roth M, Tym E, Mountjoy CQ, et al. CAMDEX – a standardized instrument for the diagnosis of mental disorder in the elderly with special reference to the early detection of dementia. *Br J Psychiatry* 1986; **149**: 698-709.

41. Folstein MF, Folstein SE, McHugh PR. Mini mental state: a practical method for grading the cognitive state of patients for the clinician. *J Psychiatr Res* 1975; **12**: 189-198.

42. Jobst KA, Smith AD, Barker CS, et al. Association of atrophy of the medial temporal lobe with reduced bloow flow in the posterior parietotemporal cortex in patients with a clinical and pathological diagnosis of Alzheimer's disease. *J Neurol Neurosurg Psychiatry* 1992; **55**: 190-4.

43. Jobst KA, Barnetson L, Shepstone BJ, and on behalf of OPTIMA. Accurate prediction of confirmed Alzheimer's disease and the differential diagnosis of dementia: the use of $^{99m}T_C$-HMPAO SPET and X-ray CT in medial temporal lobe dementias. *Int Psychogeriatr* 1997; **9**: 37-42.

44. Furukawa K, Barger SW, Blalock EM, Mattson MP. Activation of K^+ channels and suppression of neuronal activity by secreted β-amyloid precursor protein. *Nature* 1996; **379**: 74-8.

45. Mattson MP, Cheng B, Davis D, et al. β-amyloid peptides destabilize calcium homeostasis and render human cortical neurons vulnerable to excitotoxicity. *J Neurosci* 1992; **12**: 376-89.

46. Brorson JR, Bindokas VP, Iwama T, et al. The Ca^{2+} influx induced by β-amyloid peptide 25-35 in cultured hippocampal neurons results from network excitation. *J Neurobiol* 1995; **26**: 325-38.

47. Mattson MP, Tomaselli KJ, Rydel RE. Calcium-destabilizingand neurodegenerative effects of aggregated β-amyloid peptide are attenuated by basic FGF. *Brain Res* 1993; **621**: 35-49.

48. Ito E, Oka K, Etcheberrigaray R, Nelson TJ, McPhie DL, Tofel-Grehl B, et al. Internal Ca^{2+} mobilization is altered in fibroblasts from patients with Alzheimer's disease. *Proc Natl Acad Sci USA* 1994; **91**: 534-8.

49. Goodman Y, Mattson MP. K^+ channel openers protect hippocampal neurons against oxidative injury and amyloid β-peptide toxicity. *Brain Res* 1996; **706**: 328-32.

50. Drukarch B, Kits KS, Van der Meer EG, et al. 9-amino-1,2,3,4-tetrahydroacridine (THA), an alleged drug for the treatment of Alzheimer's disease, inhibits acetylcholinesterase activity and slow outward K^+-current. *Eur J Pharmacol* 1987; **141**: 153-7.